

Grindability of differentiated overburden with incorporating possibility to the Caron process

Molibilidad del escombro diferenciado con posibilidad de incorporación al proceso Caron

Yunior Correa-Cala¹, Eliveydis Mosqueda-Pérez², Yabriel Oliveros-Silvente², Roger Samuel Almenares-Reyes¹, Hugo Javier Angulo-Palma^{2*}

¹University of Moa, Holguín, Cuba.

²Nickel Research Center, Moa, Holguín, Cuba.

*Corresponding author: hangulo@cil.moa.minem.cu

Abstract

The supply of lateritic overburden with nickel content lower and close to 0.9% - called differentiated overburden- constitutes a possible technological variant in the Caron process. The purpose of this research is determining the kinetic behavior of the grinding of the differentiated overburden, with the possibility of incorporating to the Caron process in Cuba, using the facilities of the conventional Bond mill of the Nickel Research Center. It was obtained that oxides and oxy-hydroxides of iron and aluminum minerals mixed with serpentines, prevail in the ore with Ni percentages of 0.845% and Fe of 40.50% that allow classifying it as differentiated overburden. The kinetic analysis of overburden milling process showed that the specific breakage rates are in the range of 0.89 min⁻¹ to 0.20 min⁻¹, with the highest values corresponding to the larger size fractions. The **C** and **n** parameters of the cumulative kinetic model resulted in 0.056738 and 0.384293 respectively, with a coefficient of determination higher than 88%.

Keywords: differentiated overburden, grinding kinetics, Caron process

Resumen

El suministro de escombro laterítico con contenido de níquel inferior y cercano a 0,9 % -llamado escombro diferenciado- constituye una variante tecnológica posible en el proceso Caron. El propósito de esta investigación fue determinar el comportamiento cinético de la molienda del escombro diferenciado, con posibilidad de incorporación al proceso Caron en Cuba, usando para ello las instalaciones del molino convencional de Bond del Centro de Investigaciones del Níquel. Se obtuvo que en la mena prevalecen los óxidos

y oxi-hidróxidos de minerales de hierro y aluminio mezclados con serpentinas, con porcentajes de Ni de 0,845% y de Fe de 40,50% que permiten clasificarlo como escombros diferenciados. El análisis cinético del proceso de molienda del escombros mostró que las tasas de rotura específicas oscilaron en el intervalo de 0,89 min⁻¹ a 0,20 min⁻¹, correspondiendo los valores más altos a las fracciones de tamaño mayores. Los parámetros **C** y **n** del modelo cinético acumulativo resultan en 0,056738 y 0,384293, respectivamente, con un coeficiente de determinación superior al 88%.

Palabras clave: escombros diferenciados, cinética de la molienda, proceso Caron

1. INTRODUCTION

Nickel (Ni) is a critical and strategic element currently in high demand for the production of specialty steels, aerospace alloys, and lithium-ion batteries for electric vehicles. This demand stems from its ability to enhance material properties such as durability, corrosion resistance, ductility, and thermal and electrical conductivity (Bartzas *et al.*, 2021; Mitterecker *et al.*, 2022).

The primary reserves of this metal are found in lateritic and sulfide ores. The former accounts for 72.2% of the world's nickel reserve, with its annual production share increasing from 42% to 69% from 2004 to the present, due to the gradual depletion of high-grade sulfide ores in recent years (Zevgolis & Daskalakis, 2022).

It is generally recognized that laterites are classified based on their iron (Fe) and magnesium (Mg) content into limonite and saprolite zones. The uppermost layer and the base of the deposit are typically not processed due to their lowest nickel content. The zones with the greatest extraction potential are the limonite, saprolite, and transitional zones, with nickel contents exceeding 1.5% in saprolites and below this value in limonites (Díaz-Bello, 2016).

To process lateritic ores, chemical methods such as hydrometallurgy and pyrometallurgy are recommended to induce changes in their initial mineralogy, with the Caron process being one of the most important (Oxley & Barcza, 2013; Pintowantoro *et al.*, 2021).

Caron technology combines pyro- and hydrometallurgical processes (Angulo-Palma *et al.*, 2022). Among its basic sections is the grinding process, which significantly impacts its techno-economic indices due to the high energy consumption of the comminution operation (Coello-Velázquez, 2015). Laborde-Brown *et al.* (2004) identify grinding as one of the main energy

consumers among the other processes in the carbonate-ammonia technology, a reason that justifies implementing actions aimed at achieving increasingly favorable energy indicators.

Cuban lateritic ore is multicomponent, with its principal minerals belonging to the serpentinite and limonite groups. Its grinding performance is determined by the content of each mineral in the initial ore, and each component grinds according to its own individual patterns without any perceived interaction between them (Coello-Velázquez *et al.*, 2008).

Currently, the limonitic ore exhibits a high degree of depletion, caused by irrational mining practices by production companies over more than 30 years. This has led to several issues, including increased transport distances, a decrease in valuable mineral content, an increase in the content of minerals detrimental to metallurgical processes, and a continuous rise in mining costs (Sariol-López *et al.*, 2011).

One proposed solution to address this problem is to formulate blends using serpentinite minerals and "differentiated overburden" (escombro diferenciado), the latter being defined as the layer overlying the limonitic ore with a lower nickel content, typically around 0.9% (Véliz-Jardinez & Miranda-López, 2022). This proposal is based on the potential synergy achieved by formulating blends that ensure stability in the iron content, one of the parameters influencing extraction efficiency as recommended by Caron (1950).

Given the feasibility of incorporating differentiated overburden as a raw material in the Caron process, it is necessary to determine the kinetic behavior of the grinding of these resources, which is the primary justification for this investigation.

2. MATERIALS AND METHODS

For the experimental study, a sample of differentiated overburden from the typical oxide lateritic profile was used. From an initial 20-ton sample from the Camarioca Este deposit, a 500 kg sample was prepared using simple random probabilistic sampling. During sample preparation, it was ensured that the material was dry, had a maximum particle size of less than 3.15 mm, and a homogenization degree greater than 95%.

The investigation was conducted in a standard Bond mill, 305 mm in length and 305 mm in diameter, operating at 70 rpm with a steel ball charge of 20.276 kg (Figure 1). The ore charge added to the mill corresponded to a volume of 700 cm³, with grinding cycles ranging from 0.5 to 5 revolutions.

The mill simulated the equilibrium of a continuous operation with a 250% recirculation load.

The chemical elements of the ore feed to the mill were determined using Atomic Absorption Spectrophotometry (AAS), model SOLAR 929, with a flame-hydride generator. The mineralogical phases were identified by Powder X-Ray Diffraction (XRD) using a PANalytical X'PERT3 diffractometer with a Goniometer scan over an angular range from 4.0042° to 79.9962° 2θ , a step size of 0.0080° 2θ , an operating voltage of 40 kV, a current of 30 mA, and a calibration verified with an external silicon standard.



Figure 1. Experimental Bond mill setup.

3. RESULTS AND DISCUSSION

3.1. Chemical-Mineralogical Characteristics of the Initial Sample

The chemical characteristics of the initial sample (Table 1) confirm that the overburden used in the study meets the established criteria to be classified as "differentiated," as it exhibits a nickel percentage lower than and close to 0.9%—the cut-off point required by the Caron process (Angulo *et al.*, 2024)—Fe values exceeding 40%, and low contents of SiO_2 and MgO . Furthermore, the high Al_2O_3 content (12.29%) constitutes a characteristic feature of the deposit from which the sample was taken, consistent with results reported by Véliz-Jardinez & Miranda-López (2022).

Table 1. Chemical composition of the initial overburden

Elements	Ni	Co	Fe	MgO	Mn	Al_2O_3	Cr	SiO_2
Content, %	0,845	0,107	40,50	2,30	0,973	12,29	1,35	6,79

The mineralogical phases of the initial differentiated overburden are shown in Figure 2. The ore is characterized by the predominance of iron oxides and oxyhydroxides, notably goethite [$\text{Fe}^{3+}\text{O}(\text{OH})$], maghemite [$\text{Fe}_{21.16}\text{O}_{31.92}$], and hematite [Fe_2O_3], as well as aluminum in the form of gibbsite [$\text{Al}(\text{OH})_3$]. Silicon and magnesium contents are expressed in secondary silicate phases such as lizardite [$(\text{Mg},\text{Fe})_3\text{Si}_2\text{O}_5(\text{OH})_4$], talc [$\text{Mg}_3\text{Si}_4\text{O}_{10}(\text{OH})_2$], and quartz [SiO_2]. Various studies (Domènech *et al.*, 2017; Tauler *et al.*, 2023; Toirac-Leyva & Rojas-Purón, 2021) are consistent with the phases identified in this study.

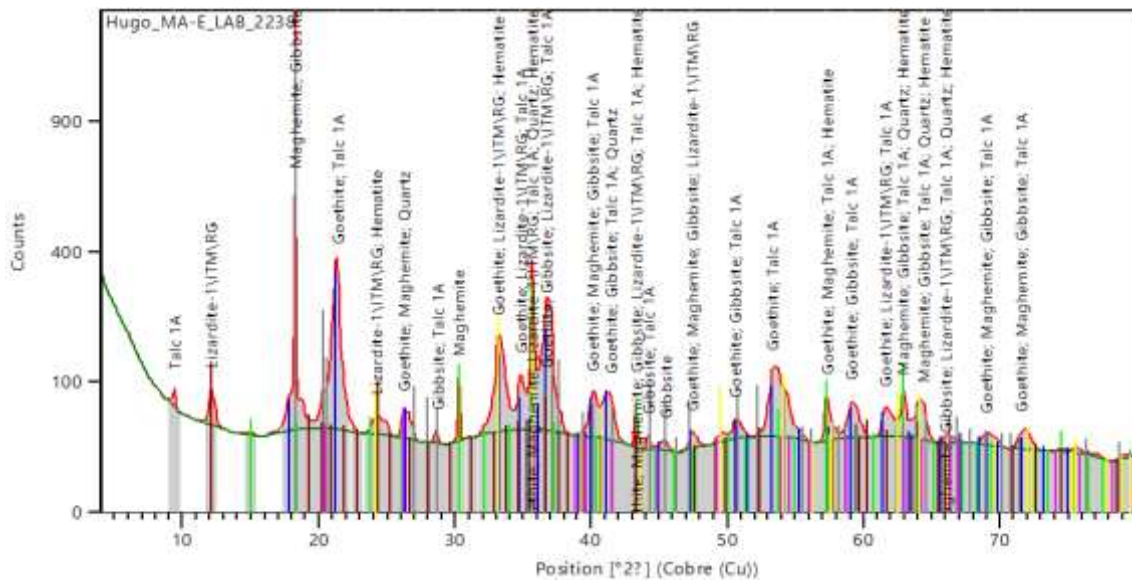


Figure 2. Mineralogical phases identified in the overburden.

3.2. Kinetics of the Differentiated Overburden Grinding Process

The particle size distribution behavior for the eight grinding times evaluated in the investigation is presented in Figure 3.

The shape of the curves confirms that fine particles predominate in all samples, regardless of the grinding time under analysis. A consistent trend is observed whereby, as the grinding period increases, the Cumulative Passing percentages (% PA) increase for each size fraction. This behavior is characteristic of an efficient comminution process.

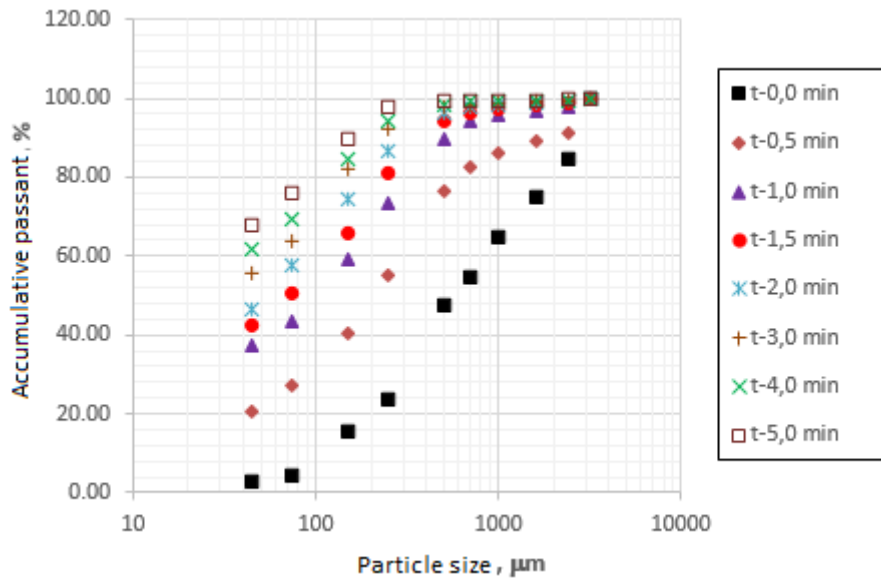


Figure 3. Particle size distribution of the overburden at different grinding times.

Based on the results from Figure 3, the specific breakage rates corresponding to each granulometric fraction were determined, considering that the material breakage velocity follows a first-order kinetic model (Table 2).

Table 2. Specific breakage rates for each particle size

Tamiz, μm	2380	1600	1000	710	500	250	150	75	45
k, min^{-1}	0,883409	0,842915	0,827518	0,808877	0,765676	0,651310	0,397009	0,252789	0,207122

Analysis of the specific breakage rate behavior across different particle sizes shows that they ranged from 0.89 min^{-1} to 0.20 min^{-1} . The highest values were found in the coarser size fractions, with a consistent decrease observed as particle size diminishes. This behavior indicates that the finer fractions are more difficult to grind, which aligns with the deductions established by Menéndez-Aguado, Coello-Velázquez & Dzioba-Blanca (2006) for clinker grinding.

The parameters C and n for the cumulative kinetic model (Figure 4) were derived from the values in Table 2, resulting in 0.056738 and 0.384293, respectively. These values are close to those reported by Namindo (2015) when investigating bituminous coal grinding. The linearization of the curve reflects a fit with a coefficient of determination greater than 0.88.

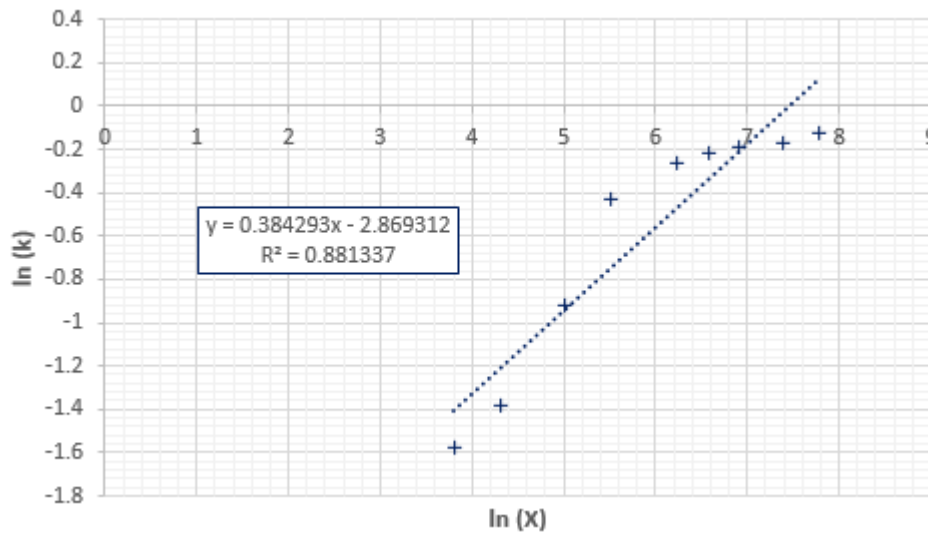


Figure 4. Determination of the C and n parameters for the cumulative kinetic model.

Finally, the cumulative kinetic model is given by Equation 1, with a form similar to that described by other authors (Menéndez *et al.*, 2006; Namindo, 2015). This model constitutes the primary novelty of the present study, as there are no prior reports on the determination of the cumulative kinetic behavior for the dry ball mill grinding of differentiated overburden.

It is also important to note that the obtained cumulative kinetic model allows for the direct estimation of the retained and accumulated mass of overburden at an industrial scale, as a function of different particle sizes and grinding times. This makes it a significant tool for energy control during the preliminary preparation of this ore for the Caron process.

$$W(x, t) = W(x, 0) \exp(-0.05673795x^{0.384293}t) \quad (1)$$

Where:

x is the particle size [μm]

t is the grinding time [minutes]

$W(x, 0)$ is the cumulative mass of rejected differentiated overburden for each particle size x before grinding [kg or tons]

$W(x, t)$ is the cumulative mass of rejected differentiated overburden at size x after grinding time t [kg or tons]

It is important to emphasize that the cumulative kinetic model for the grinding process of differentiated overburden (Equation 1) enables the estimation of the mass.

4. CONCLUSIONS

- The differentiated overburden is characterized by the predominance of mixed iron and aluminum oxide and oxy-hydroxide mineral phases, with nickel and iron percentages of 0.845% and 40.50%, respectively.
- The grinding kinetics of the differentiated overburden follow a first-order rate equation. The parameters C and n for the cumulative kinetic model are 0.056738 and 0.384293, respectively, with a coefficient of determination greater than 0.88.

REFERENCES

- Angulo-Palma, H. J., Legrá, Á. L., Urgellés, A. L., Pedrera, C. H., Gallegos, S., Galleguillos, M. F. M., & Toro, N. (2024). Use of a mixture of coal and oil as an additive for selective reduction of lateritic ore by the Caron process. *Hemijaska industrija*, 78(1), 17-27. <https://doi.org/10.2298/HEMIND230118017A>.
- Angulo-Palma, H. J., Legrá, A. L., Urgellés, A. L., Gálvez, E., & Castillo, J. (2022). Post-combustion Effect on Nickel and Cobalt Extractions from the Caron Process. In: Bindhu V., R. S. Tavares J. M., Jălu Ș. (eds), *Proceedings of Fourth International Conference on Inventive Material Science Applications. Advances in Sustainability Science and Technology*. Springer, Singapore, 515-527. https://doi.org/10.1007/978-981-16-4321-7_43.
- Bartzas, G., Tsakiridis, P. E., & Komnitsas, K. (2021). Nickel industry: Heavy metal (loid) s contamination-sources, environmental impacts and recent advances on waste valorization. *Current Opinion in Environmental Science & Health*, 21(100253), 1-9. <https://doi.org/10.1016/j.coesh.2021.100253>.
- Caron, M. H. (1950). Fundamental and practical factors in ammonia leaching of nickel and cobalt ores. *JOM-Journal of the Minerals, Metals and Materials Society*, 2, 67-90. <http://dx.doi.org/10.1007/BF03398981>.
- Coello-Velázquez, A. L. (2015). Procedimiento para la determinación de la carga circulante en circuitos cerrados de trituración y molienda. *Minería & Geología*, 31(2), 66-79.
- Coello-Velázquez, A. L., Menéndez-Aguado, J. M., & Laborde-Brown, R. (2008). Grindability of lateritic nickel ores in Cuba. *Powder technology*, 182(1), 113-115. <https://doi.org/10.1016/J.Powtec.2007.05.027>.

- Díaz-Bello, S. C. (2016). *Modelamiento cinético del procesamiento de minerales lateríticos de níquel por vía pirometalúrgica*. (Tesis Doctoral, Universidad Nacional de Colombia). 121 p.
- Domènech, C., Galí, S., Villanova-de-Benavent, C., Soler, J. M., & Proenza, J. A. (2017). Reactive transport model of the formation of oxide-type Ni-laterite profiles (Punta Gorda, Moa Bay, Cuba). *Mineralium Deposita*, 52(7), 993-1010. <https://doi.org/10.1007/s00126-017-0713-0>.
- Laborde-Brown, R. (2004). Diagnóstico energético en el proceso de molienda de la laterita. *Minería & Geología*, 20(3-4), 107-113.
- Menéndez-Aguado, J. M., Coello-Velázquez, A. L. & Dzioba-Blanca, R. (2006). Process models for simulation of Bond tests. *Mineral Processing and Extractive Metallurgy (Trans. Inst. Min Metall. C)*, 115(2), 1-7. <https://doi.org/10.1179/174328506X99925>.
- Mitterecker, J., Košević, M., Stopic, S., Friedrich, B., Panić, V., Stevanović, J., & Mihailović, M. (2022). Electrochemical investigation of lateritic ore leaching solutions for Ni and Co ions extraction. *Metals*, 12(2), 325. <https://doi.org/10.3390/met12020325>.
- Namindo, M. N. (2015). *Cinética de la molienda del carbón bituminoso*. (Trabajo de Diploma, Instituto Superior Minero Metalúrgico de Moa). 100 p.
- Oxley, A., & Barcza, N. (2013). Hydro-pyro integration in the processing of nickel laterites. *Minerals Engineering*, 54, 2-13. <https://doi.org/10.1016/j.mineng.2013.02.012>.
- Pintowantoro, S., Widyartha, A. B., Setiyorini, Y., & Abdul, F. (2021). Sodium thiosulfate and natural sulfur: novel potential additives for selective reduction of limonitic laterite ore. *Journal of Sustainable Metallurgy*, 7(2), 481-494. <https://doi.org/10.1007/s40831-021-00352-4>.
- Sariol-López, E., Otaño-Noguel, J., & Belete-Fuentes, O. (2011). Procedimiento para estabilizar la calidad del mineral que se suministra al proceso metalúrgico en la planta niquelífera Pedro Soto Alba, Moa Nickel, SA. *V Simposio Geología, Exploración y Explotación de las Lateritas Niquelíferas*.
- Tauler, E., Galí, S., Villanova-de-Benavent, C., Chang-Rodríguez, A., Núñez-Cambra, K., Khazaradze, G., & Proenza, J. A. (2023). Geochemistry and Mineralogy of the Clay-Type Ni-Laterite Deposit of San Felipe (Camagüey,

Cuba). *Minerals*, 13(10), 1281.

<https://doi.org/https://doi.org/10.3390/min13101281>.

Toirac-Leyva, V., & Rojas-Purón, A. (2021). Caracterización mineralógica de perfiles lateríticos del sector 048 en el yacimiento Punta Gorda, Holguín, Cuba. *Ciencia & Futuro*, 11(4), 23-37.

Véliz-Jardines, A. I., & Miranda-López, J. (2022). Desarrollo de investigaciones sobre la tecnología Caron durante el procesamiento de las lateritas de baja ley de níquel y de los escombros lateríticos, clasificados como: menas o minerales no industriales. *Tecnología Química*, 42(2), 361-383.

Zevgolis, E. N., & Daskalakis, K. A. (2022). The Nickel Production Methods from Laterites and the Greek Ferronickel Production among Them. *Materials Proceedings*, 5(1), 104.

<https://doi.org/10.3390/materproc202100510>.

Additional Information

Conflict of Interest

The authors declare no conflicts of interest.

Author's Contributions

YCC: Sample management and preparation, experimentation, results evaluation, and article writing; review and approval of the final version. **EMP** and **YOS:** Experimentation; article drafting, review, and approval of the final version. **RSAR** and **HJAP:** Research management, experimentation, results evaluation, and article writing; review and approval of the final version.

ORCID

YCC: <https://orcid.org/0000-0003-2934-0001>

EMP: <https://orcid.org/0009-0009-5535-9532>

YOS: <https://orcid.org/0009-0001-4873-9299>

RSAR: <https://orcid.org/0000-0002-7185-7330>

HJAP: <https://orcid.org/0000-0002-5012-0348>

Received: 11/01/2025

Accepted: 28/02/2025